JOURNAL OF EXPERIMENTAL AND THEORETICAL PHYSICS, 2024, Vol. 165, No. 3, pp. 398–406

ORDER, DISORDER AND PHASE TRANSITIONS IN CONDENSED MEDIA

SPIN-FLOP TRANSITION, INDUCING THE MAGNITOSTRICTION AND DIELECTRIC ANOMALIES IN α-MnS SINGLE CRYSTAL

© 2024 G.M. Abramova *, A.L. Freidman, S. A. Skorobogatov, A. M. Vorotynov, S. M. Zharkov, M. S. Molokeev, A. I. Pankrats

Kirensky Institute of Physics, Krasnoyarsk Scientific Center, Siberian Branch of the Russian Academy of Sciences, Krasnoyarsk 660036, Russia

** e-mail: agm@iph.krasn.ru*

Received September 16, 2023

Revised October 24, 2023

Accepted October 24, 2023

Abstract. The first experimental investigation of the magnetic and magnetistriction properties of the alfa-manganese monosulphide (α-MnS) with the cubic (NaCl-type) structure and antiferromagnetic transition at T=150 K are presented in the temperature range of 4.2–300 K at applied magnetic field up to 90 kOe. It is found, that the field dependences of the magnetization and longitudinal magnitostriction of the α-MnS single crystal have an anomalies, which are correlated with the anomalies of its dielectric permittivity. The spin-flop (SF) transition with $H_{sf} \sim 50$–70 kOe governed by the magnetic easy-plane anisotropy was observed in the temperature range below 130 K. Isotermal investigations show that the longitudinal magnetostriction and dielectric permittivity in external magnetic fields reveal its value change of 10^{-3} at Hsf.

Keywords: *order*, *disorder*, *and phase transition in condensed system*

DOI: 10.31857/S00444510240309e5

1. INTRODUCTION

Intensive research of 3*d*-element compounds (MnO, α-MnS, NiO), with face centered cubic (FCC) structure of NaCl-type (space group $Fm\bar{3}m$, centrosymmetric lattice) is caused by the discovery of a number of their physical properties, important for the development of magnonics and streintronics, such as spin-phonon interaction, hybridisation of phonon and magnon modes, size effects, spin-flop transition [1–9].

Three structural modifications of manganese monosulfide are known [10], among which only the alpha phase (α-MnS) is isostructural and isomagnetic to the oxides MnO and NiO. Substances of MnO group are collinear antiferromagnets of the second type with FCC lattice of NaCl-type [11, 12]. The antiferromagnetic transition in α-MnS at the Neel temperature $T_N = 150$ K is accompanied by rhombohedral distortion of the FCC lattice [13–16], which in the case of MnO is confirmed by infrared spectroscopy. In contrast to MnO [17], no NaCl-type lattice distortion was detected in α-MnS with similar crystal and magnetic structure by infrared spectroscopy [18]. However, the study of α-MnS and its solid solutions by Mössbauer spectroscopy [19, 20] revealed a local distortion of octahedral positions of the FCC lattice in the antiferromagnetic state. In the region of magnetic transition, an anomaly of the temperature coefficient of lattice expansion was found [21], confirming the relationship between magnetic and structural properties α-MnS. A change in the electrical and dielectric properties of the crystal α-MnS in the magnetically ordered phase was found in [22, 23]. One of the possible mechanisms explaining the relationship between electrical, dielectric, magnetic and structural properties is the exchange-striction mechanism, the importance of which for compounds of the type MnO, α-MnS and NiO was discussed in [11–13, 24–27]. The magnetostriction of α-MnS has not been previously studied except for its solid solutions $Fe_xMn_{1-x}S$ [28], the temperature dependences

of the magnetization of α-MnS have been investigated in magnetic fields up to 50 kOe [23]. The possibility of spin-flop transition in the compound MnO was first considered in [29]. The results of experimental studies for polycrystal MnO and for single crystal NiO are presented in [30] and [8].

This paper presents the results of an experimental study of the effect of strong magnetic fields up to 90 kOe on the magnetization and longitudinal magnetostriction of a single crystal α-MnS. When magnetizing the crystal along the axis [100] in the region $T < 130$ K, a jump in magnetization due to the spin-flop transition is found, which is caused by magnetic anisotropy in the easy plane. Investigations of longitudinal magnetostriction and relative dielectric constant showed that both parameters experience anomalies at the spin-flop transition.

2. SAMPLES AND EXPERIMENTAL PROCEDURES

The technology of synthesis of single crystal of manganese alpha-monosulfide (α-MnS) is presented in [31]. The samples were explored by X-ray diffraction in the range 100-300 K. X-ray diffraction pattern of the powdered sample α-MnS were obtained on a D8-ADVANCE diffractometer (K_α - radiationCu) using a VANTEC linear detector. Experiments were performed using an Anton Paar TTK450 temperature chamber. Calculations and processing of experimental data arrays were performed using the DDM programme [32]. Refinement of the cell parameters, scale factor, profile parameters and zero offset was performed. Experimental (dots) and theoretical (solid lines) X-ray diffraction patterns of the investigated sample α-MnS at $T = 300$ K are shown in Fig. 1.

It was found that at this temperature the crystal structure of the substance corresponds to a FCC lattice of the type NaCl (space group $Fm\bar{3}m$) with the unit cell parameter $a = 5.224(7)$ Å, the result agrees with tabular data (International Centre for Diffraction Data, 2016, Card 00-006-0518 green) and the results of [13, 14]. No additional structural lines were found in the X-ray diffraction patterns indicating the presence of impurity phases. The microstructure of the single crystal α-MnS and its elemental chemical composition were investigated

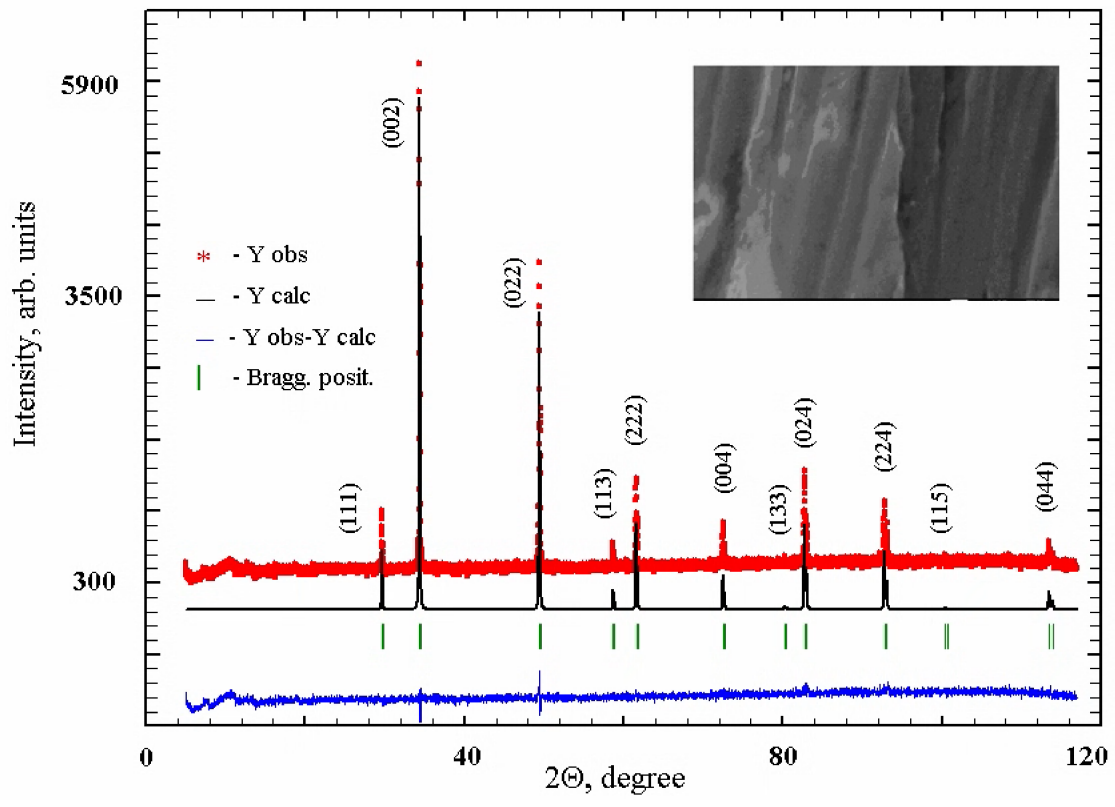

Fig. 1. X-ray diffraction patterns of single crystal α-MnS at $T = 300$ K: experimental (dots) and theoretical (solid lines). Inset: SEM-scan of the crystal surface

by scanning electron microscopy (SEM) and EDS on JEOL JSM-7001F equipment with an X-ray dispersive spectrometer (Oxford Instruments). The inset of Fig. 1 shows one of the SEM scans of the sample (resolution 100 nm). Both sides of the plane-parallel single crystal plate were examined at different points on the surface. Based on the results of analyses of more than 10 measured spectra, it is concluded that there are no additional impurities in the sample and the composition of the sample α-MnS corresponds on average to the content of $Mn_{0.992}S_{1.008}$. The original single crystal had the shape of a parallelepiped with faces coinciding with the (100) lattice planes of the NaCl type and was subsequently divided into three parts, each of which was further used for measuring dielectric ($2\times3\times1$ mm^3), magnetic (2×2×1 mm^3), resonance and magnetostriction properties ($2\times2\times7$ mm^3). Magnetostriction measurements were carried out on a capacitive dilatometer [33], developed on the basis of the PPMS measuring equipment, which allows measuring magnetostriction and linear thermal expansion coefficient at temperatures from 1.85 to 350 K, magnetic fields up to 90 kOe. Longitudinal magnetostriction was measured in a magnetic field applied along the [100] direction of the sample. The temperature of the measuring cell was kept constant during field measurements with an accuracy of ±0.5°. The parasitic capacitances of the connecting wires and the measuring cell were taken into account. The relative error of measurement did not exceed 5 %. Magnetisation measurements were performed on a PPMS-9T magnetometer in the temperature range 4.2-300 K in magnetic fields up to 90 kOe for magnetic field orientation $H \parallel [100]$. Measurement of dielectric permittivity ε_r was performed using an Agilent Technologies E4980A RLC meter. A silver-filled epoxy-based conductive glue was applied to the opposite planes of the plate with a thickness of $d = 1$ mm. For dielectric permittivity measurements ε_r , an alternating ($f = 100$ kHz) electric field $E = 1600$ V/m was oriented in the [010] direction and perpendicular to the magnetic field $H \parallel [100]$. To confirm the repeatability of the results, cyclic measurements of magnetization and magnetostriction in the magnetic field were performed repeatedly at each given temperature.

3. RESULTS AND DISCUSSION

Fig. 2 shows the field dependences of the magnetization of the crystal α-MnS , measured at temperatures of 200 and 300 K in magnetic fields up to 90 kOe (here *3* - data of [23]).

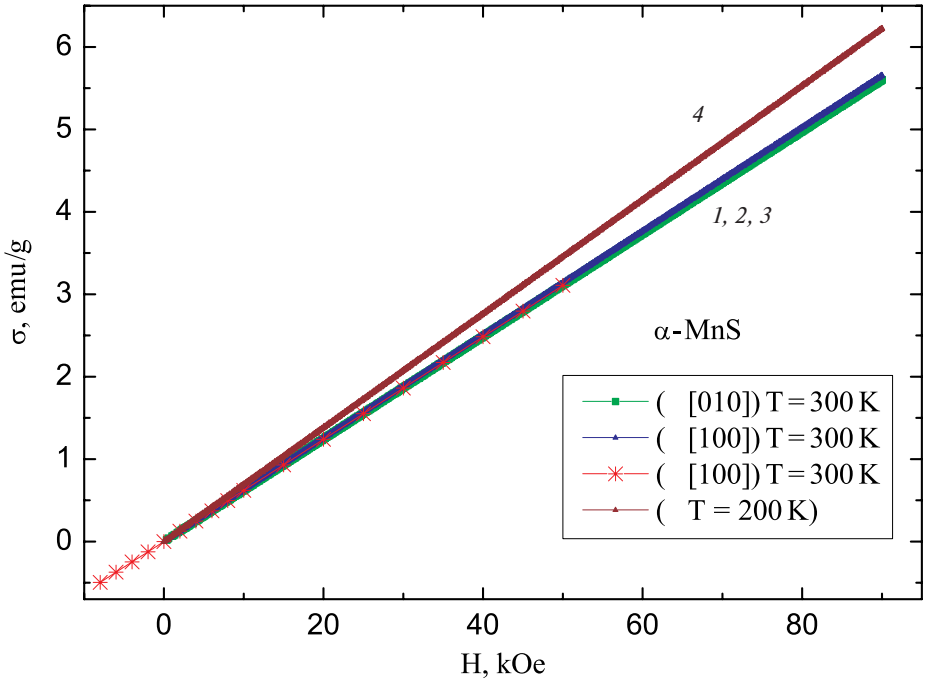

Fig. 2. Field dependences of the magnetization of single crystal α-MnS, measured at $T = 300$ K (*1*, *2* - data of the present work, and *3* - [23]) and $T = 200$ K (*4*)

In the temperature range $T \geqslant 150$ K, the magnetization of the crystal α-MnS has a linear dependence typical for paramagnets. Temperature dependences of magnetic susceptibility for the studied single crystal α-MnS , measured in magnetic fields up to 50 kOe, are given in [23]. The data obtained are close to the results of [14, 34]. At temperatures above the Neel temperature, the inverse magnetic susceptibility $1/\chi(T)$ of single crystal α-MnS (Fig. 3) corresponds to the Curie-Weiss law with negative paramagnetic Curie-Weiss temperature $\Theta = -520 \pm 5$ K and effective magnetic moment $\mu_{eff} = (5.93 \pm 0.01)\mu_B$. The given experimental values Θ and μ_{eff} are averaged over the whole series of measurements in different fields. The obtained value of the effective magnetic moment μ_{eff} agrees with the theoretical value $5.916\,\mu_B$ with the values, $g = 2$, $S = 5/2$.

The values of the Neel temperature T_N and the paramagnetic Curie-Weiss temperature Θ allow to estimate the parameters of 180-degree and 90-degree exchanges $J_2(180^\circ) = -4.2$ K, $J_1(90^\circ) = -5.3$ K using the known relations [35] for antiferromagnets with FCC lattice and magnetic ordering of the second type:

$$k_B T_N = -(2/3)S(S+1)6J_2$$

and

$$k_B\Theta = (2/3)S(S+1)[12J_1 + 6J_2]$$

with the Hamiltonian of the exchange interaction

$$H = 2J_1\sum_{i=1}^{12} S_i S_{i+1} + 2J_2\sum_{j=1}^{6} S_j S_{j+1},$$

where the summation for i is for the nearest 12 neighbours and for j is for the 6 second neighbours.

The type II magnetic ordering in the FCC lattice and the corresponding exchange integrals J_1 and J_2 are shown in Fig. 4.

In [14, 16] it was suggested that in the region $T_S = 130$ K in manganese monosulfide with FCC structure (α-MnS) at decreasing temperature a rhombohedral contraction of the crystal lattice is replaced by a rhombohedral elongation.

As a result of experimental studies, it was found that in the magnetically ordered state, the field dependences of the magnetization and magnetostriction of the α-MnS crystal differ significantly in the temperature regions above and below 130 K.

In the region 130-150 K, the field dependences of the magnetization σ (H) of the single crystal α-MnS retain a linear character in fields up to 90 kOe. The magnitudes of longitudinal magnetostriction $\lambda_{\|}$ in magnetic fields up to 90 kOe in this temperature range are typical for isostructural and isomagnetic

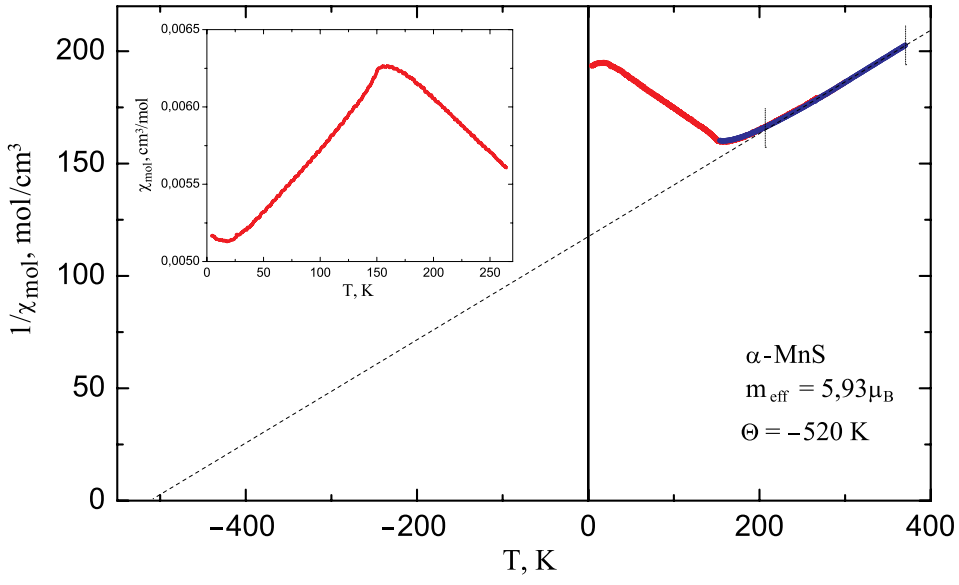

Fig. 3. Temperature dependence of the inverse molar susceptibility of single crystal α-MnS, measured in a magnetic field of $H = 500$ Oe (red) and 30 kOe (blue). Vertical lines show the linear section on the temperature dependence of the inverse molar susceptibility. Inset shows the temperature dependence of the direct molar susceptibility of the single crystal α-MnS

compounds MnO, NiO [36, 37] and do not exceed the values of $\lambda_{\|} = +(1 \pm 0.5) \cdot 10^{-5}$. The mechanism of magnetostriction changing in isostructural antiferromagnetics MnO, NiO has been repeatedly discussed in the literature [11, 12, 16, 36, 37] and associated with the formation of a complex domain structure including magnetic S- and structural T-domains. At temperatures below $T_S = 130$ K, the magnetic and magnetostrictive properties of single crystal α-MnS – change dramatically. It has been found that when changing the magnetic field in the range from -90 kOe to 90 kOe in the region of the critical magnetic field $\pm H_c$, a jump-like and reversible changing in the magnetization $\pm\sigma(H)$, accompanied by magnetic hysteresis, is observed. Fig. 5 shows the field dependences of the magnetization of the crystal α-MnS, measured at magnetic fields up to 90 kOe at different temperatures.

The experimental results, in particular, the difference in the magnitudes of magnetic susceptibility before and after the transition, as well as the presence of hysteresis indicate that at a given temperature in the region $H_c = H_{sf}$ single crystal α-MnS undergoes a magnetic transition of spin-flop type. When the sample is cooled to the temperature of liquid helium, a decrease in the value of $H_c = H_{sf}$ from about 70 kOe for $T = 100$ K to about 50 kOe at 4.2 K with a simultaneous increase in the magnetization jump value is observed. From the experimental results presented above, it follows that the critical field $H_{sf} \sim 50$ kOe found at $T = 4.2$ K for the crystal α-MnS, is almost identical to the spin-flop transition field in NiO [8] and MnO [30]. The experimentally detected spin-flop transition in NiO ($H_{sf} = 54$ kOe at $T = 5$ K) is explained [8] within the framework of the model [29] by the rotation of the magnetic moments of nickel ions in planes of (111) type perpendicular to the trigonal ⟨111⟩, axis from the $[11\bar{2}]$ direction to the $[1\bar{1}0]$ direction. In contrast to NiO [8] and MnO [30], in which the presence of spin-flop transition was fixed by indirect signs (from the analysis of temperature dependences of magnetic susceptibility in polycrystalline samples [30] or from field dependences of field derivatives of magnetization for single crystal [8]), in α-MnS the field dependences of magnetization (Fig. 5) have a classical spin-flop shape manifested as a jump of the magnetization in the critical field region.

We discuss the nature of the spin-flop transition observed in the crystal α-MnS in a magnetic field

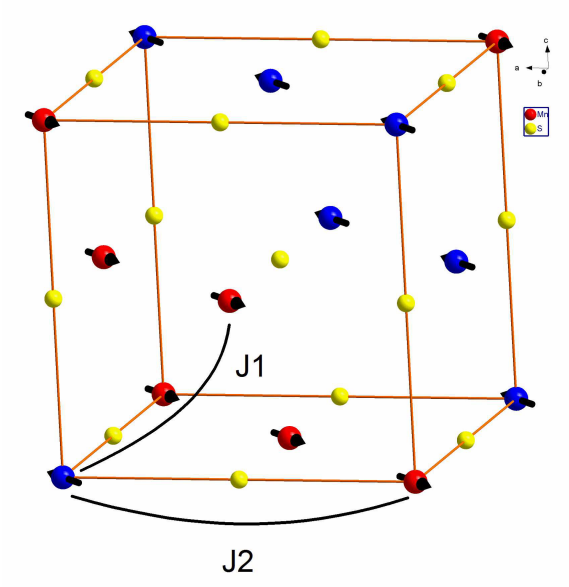

Fig. 4. Crystallographic cell of α-MnS with magnetic ordering of the second type. The exchange paths $J_2(180^\circ)$ and $J_1(90^\circ)$ through sulphur ions are shown. Manganese ions belonging to different sublattices are indicated in blue and red colours

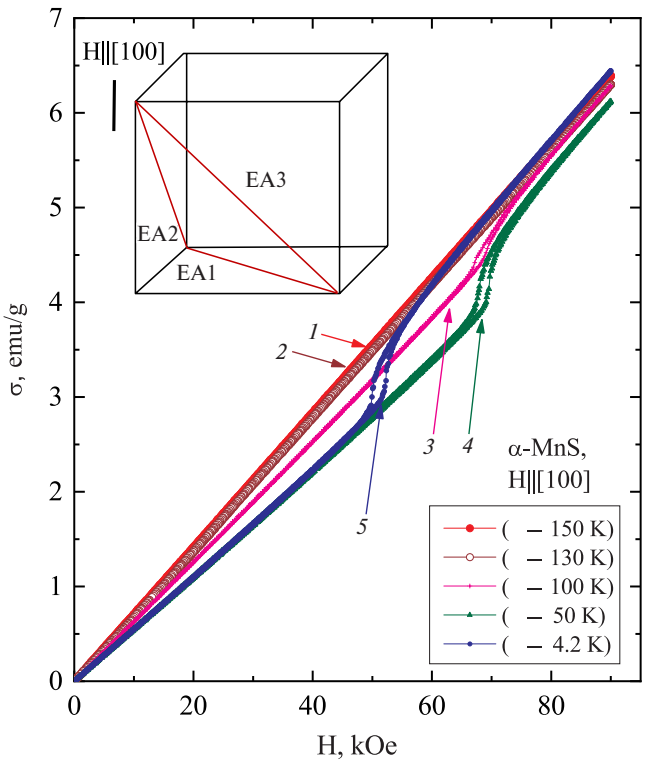

Fig. 5. Field dependences of the magnetization of the single crystal α-MnS, measured at different temperatures. Inset: three possible directions of the easy axes (EA) of ⟨110⟩ type in a FCC lattice of NaCl type are labelled by the numbers *1*, *2*, 3.

at $H \parallel [100]$. As a result of neutronographic studies [16, 21, 38] at $H = 0$, it was found that the magnetic structure of α-MnS at $T = 4.2$ K is described within the framework of a representation that takes into account the direction of the propagation vector of the antiferromagnetic structure $\mathbf{Q} = k$ (1/2, 1/2, 1/2), which corresponds to the doubling of the magnetic cell relative to the crystallographic cell and highlights the direction of rhombohedral deformation of the cubic lattice $\langle 111 \rangle_Q$. In magnetic planes of the type (111), perpendicular to the direction ⟨111⟩, the magnetic moments of the ions Mn^{2+} are oriented along the axes of $[1\,\bar{1}0]$ type.

The analysis of the experimental data presented above is performed under the assumption that α-MnS similarly to MnO and NiO is an easy plane (EP) antiferromagnet, in which a complex domain structure consisting of structural T-domains and magnetic S-domains is formed as a result of rhombohedral distortions. Due to the cubic symmetry of the paramagnetic state in a real crystal, four directions of rhombohedral distortions ⟨111⟩ are possible, which causes the formation of structural T-domains of four types. Perpendicular to the direction of distortion ⟨111⟩ there are ferromagnetically ordered planes of the type (111), which are EP of anisotropy. Neighbouring planes (111) are coupled by the antiferromagnetic exchange. The inset of Fig. 5 shows such a plane (111) for one of the four possible T-domains. Due to weak trigonal anisotropy in EP, there are three possible directions easy anisotropy axes of $\langle 1\,\bar{1}0 \rangle$ type. Since the plane contains three such directions, labelled EA_1, EA_2 and EA_3, in the region of the crystal occupied by one T-domain, three types of magnetic S-domains with different directions of the antiferromagnetic vector $\mathbf{L} = \mathbf{M}_1 - \mathbf{M}_2$ are formed. When magnetizing along one of the easy anisotropy axes (EA_1, EA_2 or EA_3), the spin-flop transition is accompanied by a rotation of the vector **L** from the direction of the corresponding EA (e.g. $[1\,\bar{1}0]$ for EA_1) to the difficult axis $[\bar{2}11]$. Obviously, when the $\mathbf{H} \parallel [100]$ field is oriented in a magnetic domain with EA_1, the spin-flop transition does not occur, since the vector **L** is already perpendicular to the field direction **H**, and the field dependence of the magnetization in this domain is determined by the magnetic susceptibility $\chi_\perp$. In other S-domains with EA_2 and EA_3 antiferromagnetic vectors make the same angle $\pi/4$ with the field direction, and the field dependences of the magnetization in these domains in the field region $H < H_{sf}$ are determined by the superposition of susceptibilities $\chi = (\chi_\perp + \chi_\parallel)/2$.

Within the framework of pseudocubic lattice symmetry, the EP of the other three types of T-domains are superimposed with the initial EP shown in the inset of Fig. 5, by successive rotations by an angle $\pi/2$ around the field direction $\mathbf{H} \parallel [100]$. This explains why for this field direction, despite the presence of T-domains, the spin-flop transition occurs simultaneously at the same value of H_{sf}^{100} for all T-domains and therefore has a well-defined shape.

Thus, the magnetization jump observed at the magnetic field orientation $\mathbf{H} \parallel [100]$ is a reflection of the spin-flop transitions occurring in the S-domains with EA_2 and EA_3. And the true critical field H_{sf} transitions for these directions can be defined as the projection of the corresponding critical field H_{sf}^{100} onto EA_2 and EA_3. Hence, the true value of the critical field of the spin-flop transition in the EPfor the [100] direction is $H_{sf} = H_{sf}^{100} \cos(\pi/4) = 36.2$ kOe at $T = 4.2$ K. This value allows to define the effective field of anisotropy in the EP as $H_{A3} = H_{sf}^2/2H_E$. The value of the effective exchange field required for these calculations can be estimated from the field dependence of the magnetization for the region $H > H_{sf}$ (Fig. 5), where the magnetization is determined by the magnetic susceptibility $\chi_\perp = M_0/H_E$ [39], where M_0 is the magnetization of the antiferromagnetic sublattices. Thus, the spin-flip of antiferromagnetic sublattices occurs at the magnetic field $H = 2H_E$. From the experimental value $\chi_\perp = 7.15 \cdot 10^{-5}$ cm^3/g and the saturation magnetization $M_S = 5\mu_B$/ f. u. for the Mn^{2+} ion, the value of the exchange field $H_E = 2.2 \cdot 10^6$ E (or 297 K) is obtained. Using this parameter, we obtain the effective anisotropy field in the EP of the crystal α-MnS at $T = 4.2$ K as $H_{A3} = 290$ Oe. If we compare it with the anisotropy field with respect to the main axis of anisotropy $\langle 111 \rangle H_{A1} = 12.5$ kOe (obtained from the gap for the high-frequency branch of antiferromagnetic resonance $\omega_c = 22$ sm^{-1} [18]), this relation looks typical for the EP antiferromagnets, in which the anisotropy in the EP is determined by higher-order invariants than the anisotropy with respect to the main axis of the crystal. At the same time, the absolute value of the field H_{A3} turned out to be unexpectedly

large for the S-ion Mn^{2+}. This value is almost three times higher than the analogous parameter for NiO ($H_{A3} = 110$ Oe [8]), whose magnetoanisotropic properties are determined by the Ni^{2+} ion with strong spin-orbit coupling. No magnetic anisotropy in the EP at T = 77 K was detected for the single crystal MnO according to the antiferromagnetic resonance data [40]. For comparison we can still provide the effective anisotropy field $H_{A3} = 3.3$ Oe in the EP of the rhombohedral crystal $YFe_3(BO_3)_4$ [41], whose magnetic properties are also determined by the S-ion Fe^{3+}.

Taking into account that in the study of the field dependences of the magnetization of the crystal α-MnS in the temperature region 130–150 K the spin-flop transition is not manifested, we can assume that the appearance of relatively strong anisotropy in the EP at $T < 130$ K is due to the change of the sign of rhombohedral distortions of the lattice at this temperature and the strengthening of these distortions with further temperature decrease. Let us note another feature of the spin-flop transition in α-MnS. In the spin-flop state at $H > H_{sf}$, the antiferromagnetic vectors **L** in all domains are oriented perpendicular to the applied magnetic field. Consequently, the spin-flop transition actually results in monodomainisation of the crystal. However, the coincidence of the field dependences of the magnetization in the region $H < H_{sf}$ during magnetocycling suggests that the domain structure is restored during the reverse transition from the spin-flop state. The most probable reason for such reconstruction of the domain structure is that there are local (most likely growth) stresses in the crystal, the orientation of which differs in different regions of the crystal. As a result, during the transition to the ordered state in each particular region of the crystal, these stresses contribute to the selection of a certain type of domain Ti with one of the four possible axes of rhombohedral distortions of the ⟨111⟩ type. Since the application of an external magnetic field does not change these stresses, when the field is reduced and the transition from the monodomain spin-flop state to the collinear phase occurs, the initial domain structure is restored in the same way as in the transition from the paramagnetic to the magnetically ordered state. Fig. 6 shows the field dependences of magnetostriction $\lambda_{\|}$ of single crystal α-MnS, measured at temperatures 4.2, 50 and 100 K.

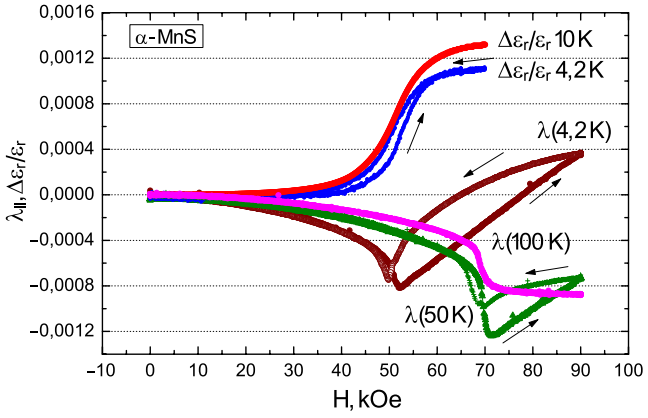

Fig. 6. Field dependences of relative permittivity ($\delta\varepsilon_r/\varepsilon_r$) and longitudinal magnetostriction $\lambda_{\|} = \delta l/l$ for the single crystal α-MnS

We note three striking features of the magnetostriction which are characteristic of the temperature region below130 K. First of all, from the comparison of the data presented in Figs. 5 and 6, it follows that in the region of the spin-flop transition there is an anomalous change of longitudinal magnetostriction $\lambda_{\|}$ in the magnetic field. The jump in magnetostriction at H_{sf} increases with decreasing temperature, similar to the jump in sample magnetization, and reaches negative values of the order of 10^{-3}, which is two orders of magnitude higher than the values observed for the sample α-MnS in the 130–150 K temperature range.

In addition, the nature of the field dependence of magnetostriction above and below the spin-flop transition differs significantly. While at $H < H_{sf}$ magnetostriction depends nonlinearly on the magnetic field, at $H > H_{sf}$ its absolute value decreases linearly with further increase in field. An interesting feature of $\lambda_{\|}(H)$ in the region above the spin-flop junction is the unusual field hysteresis observed at $T = 4.2$ and 50 K. When the field decreases from 90 kOe to H_{sf} a significantly nonlinear change in magnetostriction is observed, which almost mirrors the behaviour at the $H \leqslant H_{sf}$. Hysteresis behaviour of $\lambda_{\|}(H)$ above spin-flop transition is well reproduced by magnetocycling. Note that the value of $\lambda_{\|}(H)$ for the crystal α-MnS turned out to be an order of magnitude higher than in $Fe_xMn_{1-x}S$ [28]. We are not aware of data on the magnetostriction behaviour for MnO and NiO in strong magnetic fields.

Note that the anisotropy field estimated above in the EP of the crystal α-MnS is an effective field, which most likely contains not only the contribution

of magnetic crystallographic anisotropy, but also other contributions - primarily the contribution of growth anisotropy and the magnetoelastic contribution. Perhaps, it is the significant magnetoelastic contribution that is the reason for the unusually large value of the effective anisotropy field in the easy plane of the crystal.

Fig. 6 also shows the field dependences of the change in the real part of the dielectric permittivity ($\delta\varepsilon_r/\varepsilon_r$) measured at $T = 4.2$ K and $T = 10$ K ($f = 100$ kHz). The results indicate that the previously detected [23] change ($\delta\varepsilon_r/\varepsilon_r$) of single crystal α-MnS in the region of $H_c \sim 50$ kOe at 4.2 K correlates with spin-flop type magnetic transition and magnetostrictive process. In this case, the relative change in the magnitude of ($\delta\varepsilon_r/\varepsilon_r$) at $H = H_{sf}$ is of the order of 10^{-3}, comparable to the change in the magnetostriction magnitude $\lambda_{||}$. Since the anomalous changes of ($\delta\varepsilon_r/\varepsilon_r$) and $\lambda_{||}$ for α-MnS in the magnetic field occur simultaneously at the spin-flop transition, and also, taking into account the same order of the change of these parameters at the transition, we can assume that the magnetodielectric effect is related to the change of the magnetostriction.

4. CONCLUSION

The magnetization and magnetostriction of a single crystal α-MnS with FCC lattice of the NaCl type in a wide range of temperatures 4.2 –300 K and magnetic fields up to 90 kOe have been investigated. It was found that in the temperature range below 130 K, when changing the magnetic field oriented along the crystallographic axis [001], a magnetization jump is observed when the critical field is reached, which varies in the range 50–70 kOe as a function of temperature. It is shown that this jump is due to the spin-flop transition occurring in the easy plane (111) of the crystal and is caused by the magnetic anisotropy in this plane.

Isothermal studies of longitudinal magnetostriction and relative dielectric change at the same temperatures have shown that both characteristics reach values of the order of 10^{-3} in the fields 50–70 kOe, reveal anomalies at the spin-flop transition.

ACKNOWLEDGEMENTS

The authors are grateful to O. A. Bayukov and D. A. Balaev for fruitful permittivity of the experimental results, as well as to the center for collective use of the Federal Research Center Krasnoyarsk Scientific Center for the opportunity to perform experimental work.

REFERENCES

1. M. B.Jungfleisch, W. Zhang, A. Hoffmann, Physics Letters A, **382,** 865 (2018).
2. A.A. Bukharaev, A. K. Zvezdin, A. P. Pyatakov et al., Physics-Uspekhi, **61**, 1175 (2018).
3. A. V. Chumak, V. I. Vasyuchka, A. A. Serga et al., Nature Physics, **11(6)**, 453 (2015).
4. E. Aytan, B. Debnath, F. Kargar, et al. Apl. Phys. Let., **111**, 252402 (2017).
5. S. Palchoudhury, K. Ramasamy, R. Gupta et al., Front. Mater. **5,** 83 (2019).
6. S. Baierl, J. H. Mentink, M. Hohenleutner, et al., Phys.Rev. Let., **117**, 197201 (2016).
7. D.A. Balaev, A. A. Krasikov, S. I. Popkov et al., J.Mag. Magn.Mat., **539**, 168343 (2021).
8. F.L.A.Machado, P. R.T.Ribeiro, J. Holanda et al., Phys.Rev. B, **95,** 104418 (2017).
9. R.B.Pujary, A. C. Lokhande, A. A. Ayday et al., Materiaj & Design, **108,** 51-517 (2016).
10. C.N.R. Rao, K. P.R. Picharody, Progress in Solid State Chem. **10**, 207 (1976).
11. W. L. Roth, Journal de Physique, supplement C7, **38**, **C7-** 151 **(**1977).
12. M. E. Lines, E. D. Jones, Phys. Rev. **141**, 525 (1966).
13. B. Morosin, Phys. Rev. **B 1,** 236 (1970).
14. H.H. Heikens, G. A. Wiegers, C. F. Bruggen, Solid State Commun. **24 (3)**, 205 (1977).
15. H. van der Heide, C. F. van Bruggen, G. **A.** Wiegers, C. Haas, J. Phys. C: Solid State Phys., **16,** 855 (1983).
16. W. Kleemann, F. J. Schafer, J. Mag. Magn. Mat. **25**, 317 (1982).
17. T. R. Ch. Kant, F. Mayr, A. Loidl, Phys. Rev. **B77**, 024421 (2008).
18. J. V. Gerasimova, G. M. Abramova, V. S. Zhandun, et al., J Raman Spectrosc. **50**, 1572, (2019).
19. A. Tomas, L. Brossard, J. L. Dormann et al. J. Magn. Magn. Mater. **31**, 755 (1983).
20. G. M. Abramova, Yu. V. Knyazev, O. A. Bayukov et al., Physics of the Solid State, **63**, 68 (2021).

21. G. Abramova, Ju. Schefer, N. Aliouane, et al., J. All. Comp., **632**, 563 (2015).

22. S.S.Aplesnin, L. I.Ryabinkina, G. M.Abramova, et al., Phys. Solid State. **46**, 2067 (2004).

23. G. Abramova, A. Freydman, E. Eremin, et al., J. Supercond. Novel Magnetism, **35**, 277 (2022).

24. D. S. Rodbel, J. Owen, JAP, **35,** 1002 (1964).

25. T. Yildirim, A. B. Harris, and E. F. Shender, Phys. Rev.B **58**, 3144 (1998).

26. M.A. Carpenter, Z. Zhang, and Ch. J. Howard, J. Phys.: Cond. Matt. **24**, 156002 (2012).

27. Z. Zhang, N. Church, S.-Ch. Lappe, et al., J. Phys.: Cond. Matt. **24**, 215404 (2012).

28. G. M. Abramova, G. Petrakovskiy, R. Zuberek, et al., JETP Lett. **90,** 207 (2009).

29. F. Keeper, W. O'Sullvan, Phys.Rev.,**108**, 627 (1957).

30. D.Bloch, J. L. Feron, R. Georges, et al., JAP, **38**, 1474 (1967).

31. G.M. Abramova, A. L. Freidman, V. V. Sokolov, Patent RU 2 793 017 C1, 2023.

32. L. A. Solovyov, J. Applied Crystallography. **37**, 743 (2004).

33. A.L. Freidman, S. I. Popkov, S. V. Semenov, and others, Letters to JTP, 79 (2018).

34. J. J. Banewicz, R. Lindait, Phys. Rev., **104**, 318 (1956).

35. M. Vorotynov, G. M. Abramova, V. V. Sokolov et al., Physics of the Solid State, **54**, 2208 (2012).

36. C.R.Becker, Ph.Lau, R. Geick, V.Wager, Phys.Stat.Sol (b), **67**, 653 (1975).

37. J. **A.** Reissland, N. A. Begum, J. Phys. C (Solid St. Phys.), **2,** 874 (1969).

38. J. A. M. Paddison,M. J. Gutmann, J. Ross Stewart, et al., arXiv:1602.08420v1 [cond-mat.mtrl-sci] 26 Feb 2016.

39. P. de V. du Plessis, S. J. van Tonder, L. Alberts, J. Phys. C: Solid State Phys. **4,** 2565(1971)

40. T. R. McGuire and W. A. Crapo, J. Appl. Phys., **33**, 1291 (1962).

41. S. Steger and V. Yu. Pomjakushin, VP Report PSI, Switzerland (2008).

42. E.A. Turov, Physical properties of magnetically ordered crystals, (Academic, New York, 1965).

43. V.S.Mandel, V. D.Voronkov, D. E. Gromzin, JETF, **36**, 521 (1973).

44. A. Pankrats, G. Petrakovskii, L.Bezmatemyik, et al., Phys. Sol. State, **50**, 79 (2008).